Article

Study on the Migration and Transformation of Nitrogen in Mine Water under the Action of Water–Coal Interactions

Binbin Jiang [1,†]**, Ze Zhao** [1,2,†]**, Zhiguo Cao** [1]**, Deqian Liu** [3]**, Jiawei Tang** [1]**, Haiqin Zhang** [1]**, Yuan Liu** [1]
and Dingcheng Liang [1,2,*]

[1] State Key Laboratory of Water Resource Protection and Utilization in Coal Mining, Beijing 102299, China; 20029907@chnenergy.com.cn (B.J.); zhaoze202207@163.com (Z.Z.); zhiguo.cao@chnenergy.com.cn (Z.C.); 20062356@chnenergy.com.cn (J.T.); haiqin.zhang.c@chnenergy.com.cn (H.Z.); liuyuan990325@163.com (Y.L.)

[2] School of Chemical and Environmental Engineering, China University of Mining and Technology—Beijing, Beijing 100083, China

[3] School of Chemistry and Chemical Engineering, Anqing Normal University, Anqing 246011, China; liudeqian@aqnu.edu.cn

[*] Correspondence: liangdc@cumtb.edu.cn

[†] These authors contributed equally to this work.

Abstract: The coal pillar dam of underground reservoirs and residual coal in goaves have a direct impact on the quality of mine water. In this paper, the coal pillar dam of an underground reservoir and residual coal in the goaf and mine water in the Daliuta coal mine are used as research objects. The adsorption mechanism of residual coal with respect to NO_3^- in mine water was analyzed by carrying out adsorption experiments. The composition and variation of organic matter in mine water at different times were simulated using three-dimensional fluorescence spectrum analysis. The influence of residual coal and microorganisms in underground reservoirs on the change in NO_3^- contents in mine water was explored. Moreover, the mechanism of NO_3^- changes in the water body was clarified. The results showed that the concentration of NO_3^- in the water first decreased and then increased, showing a downward trend as a whole. The adsorption of NO_3^- by residual coal led to a decrease in its concentration, which conformed to a pseudo-second-order kinetic model and Freundlich isothermal adsorption model, indicating that the adsorption process of NO_3^- by residual coal is mainly carried out via chemical adsorption and multi-layer adsorption. The increase in NO_3^- concentration was caused by the hydrolysis of tryptophan and other protein-like substances in the water into nitrate under the action of microorganisms.

Keywords: coal mine underground reservoir; water–coal interaction; nitrogen; migration transformation

1. Introduction

The majority of China's coal production occurs in the northwest, where arid conditions and a severe lack of water resources severely impede local development. In order to safeguard mine water, there has been a switch from the "blockage method" to the "storage method", and scholars have proposed the idea of a "coal mine underground reservoir" [1,2]. This refers to the usage of underground goaves to cleanse, store, and utilize mine water. Cameira et al. [3] found that coal mine underground reservoirs can reduce the total hardness, suspended solids, and pollutant concentrations of mine water. Purified mine water can be used as groundwater and other aspects, which realizes the recycling of mine water and effectively solves the problem of mine water waste and evaporation. Engineering projects have demonstrated that mine water in coal mine underground reservoirs is mostly derived from subterranean sewage, coal mining face water, and the crack seepage of the overlying strata. The majority of this water comprises high salinity mine water (1000–10,000 mg/L), with a high nitrogen content.

As the main element in the natural environment, nitrogen is one of the most basic circulating substances in the biosphere [4]. Large nitrogen concentrations in the water

will impede the movement of nutrients and lead to the eutrophication of a body of water. Wang et al. [5] revealed that nitrogen in water mainly exists in the form of organic nitrogen and inorganic nitrogen (ammonia nitrogen, nitrite, and nitrate), and various forms of N can be converted into each other. Among them, macromolecular organic nitrogen (ORG-N) can be converted into ammonia nitrogen (NH_4^+–N) under the action of microorganisms. Ammonia nitrogen is oxidized to nitrite nitrogen (NO_2^-–N) by nitrite bacteria, and nitrite nitrogen forms nitrate ammonia (NO_3^-–N) under the action of nitrate bacteria. Zhao et al. [6] used dynamic leaching column experiments to explore the removal effect of coal gangue on ammonia nitrogen in mine water at room temperature. The results showed that the illite and kaolinite contained in coal gangue were the main reasons for the high removal ability of ammonia nitrogen in coal gangue, and the removal efficiency was 73–81%. Zhang et al. [7] simulated the pore medium of underground reservoirs using a coal gangue column to study its removal effect on NO_3^- in water. The results showed that water–rock interactions can effectively remove NO_3^- from mine water, and the removal rate was 74–90%.

Research on the removal of nitrogen from mine water by coal mine underground reservoirs is currently mostly focused on coal gangue and caving rock. The actual situation on site reveals that more than 80% of the subterranean reservoir structure of the coal mine is made up of coal pillar dams, residual coal, and numerous coal piles in addition to fallen rocks in the goaf. In addition, coal is a type of bio-organic rock, and unlike rock, it has a more complicated structural makeup. For example, coal contains dissolved organic matter (DOM). Xiong and Mladenov et al. [8,9] found that high concentrations of ammonia nitrogen in groundwater were derived from the degradation of DOM. In early studies, the removal effect and mechanism of alkali metals and sulfate ions in mine water by residual coal in the underground reservoir of a coal mine have been explored. However, the influence of coal pillar dams and residual coal on NO_3^- in mine water and the mechanism of nitrogen migration and transformation under the action of water and coal are still unknown.

Therefore, based on the water–coal coupling dynamic simulation experiment, in this paper, the reasons for the change in NO_3^- concentrations under the action of water–coal interactions and the influence of residual coal on the migration and transformation of nitrogen in the underground reservoir of a coal mine are discussed, and the mechanism of changes in nitrogen levels in the water body is expounded, which provides theoretical and experimental support for the evolution mechanism of mine water quality in the underground reservoirs of coal mines.

2. Materials and Methods

2.1. Sample Collection

The mine water at the inlet and outlet of the No. 1 reservoir in the Daliuta coal mine and the coal of the 5^{-2} coal seam were collected for experimental study, and NO_3^- was selected to characterize the hydrochemical characteristics of water bodies. The collection of water samples from the inlet and outlet of the underground reservoir of the coal mine was carried out in accordance with the Chinese standard HJ494–2009 [10] and the HJ495–2009 [11].

2.2. Dynamic Simulation

A dynamic experimental device designed to simulate the real operation state of an underground reservoir is shown in Figure 1. The coal sample was broken in advance and placed in the simulation test device, and 40 L of mine water was added to the experimental device. According to the total water storage in the underground reservoir of the coal mine to the experimental water volume ratio, the daily water intake of the experiment was determined to be 55 mL, and the water output was 70 mL. To avoid clogging the peristaltic pump, the filter was filled to filter the coal sample's residue when the orifice of the device was installed with the plastic water tank valve. Valve 2 was used for daily sampling to

analyze the change law of organic matter in the water body and to analyze the mechanism of nitrogen migration in the water body under the action of water–coal interactions.
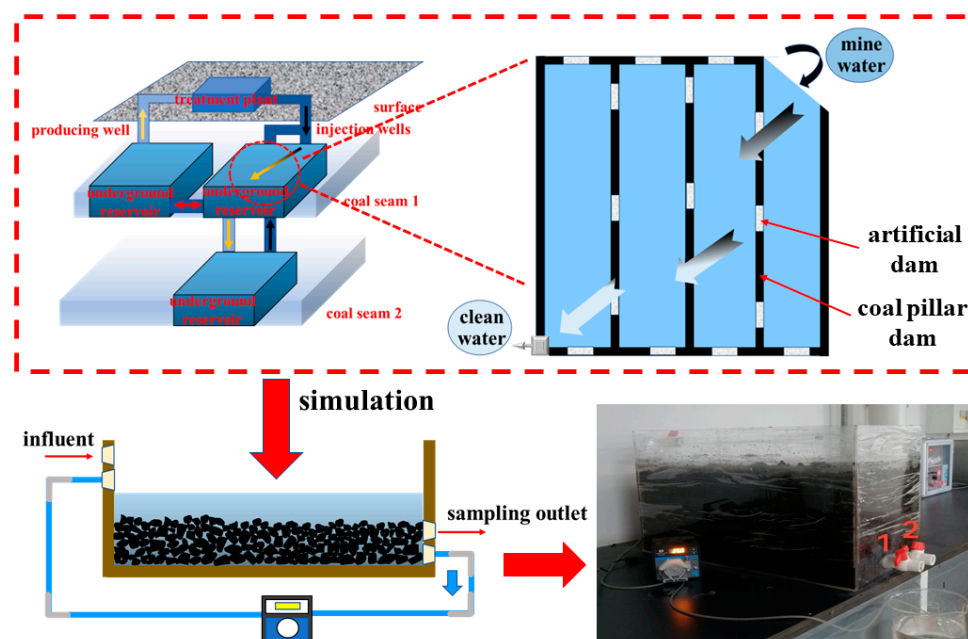
Figure 1. Coal mine underground reservoir principle and experimental device: 1 is a valve for the discharge and circulation of water in the experimental device; 2 is a valve for the sampling of water samples during the experiment.

2.3. Adsorption Experiment of the Residual Coal with Respect to NO_3^- in Mine Water

The prepared NO_3^- solution, a certain amount of pulverized coal, and mine water were placed in a centrifuge tube. Three parallel samples were set up in each group of experiments. The nozzle was sealed in a constant temperature oscillation box at 25 °C, and the oscillation speed was set to 200 r/min. After the reaction, the supernatant was collected and filtered through a 0.45 μm filter membrane to determine the concentration of NO_3^- in the mine water. The effect of residual coal on the adsorption and removal of NO_3^- in the mine water under different conditions was investigated, and the adsorption mechanism between residual coal and NO_3^- in the mine water was analyzed:

a. The effect of coal dosage on the adsorption effect of NO_3^- in the mine water: The fixed mass concentration of NO_3^- in the experiment was 20 mg/L, and coal dosages were 0, 0.05, 0.1, 0.15, 0.2, 0.25, 0.3, and 0.4 g for an oscillation time of 30 min.

b. The effect of oscillation time on the removal of NO_3^- by coal adsorption: The fixed mass concentration of NO_3^- in the experiment was 20 mg/L. The optimum coal dosage in the above experiment was selected, and the oscillation time was 0.5, 1, 2, 3, 4, 5, 8, 10, 20, 30, 40, 50, and 60 min.

c. The effect of initial NO_3^- mass concentration on coal removal rates: The optimal oscillation time and coal dosage were selected in the above experiments, and the initial mass concentration of NO_3^- was 5, 10, 15, 20, 25, 30, and 40 mg/L.

The adsorption capacity of NO_3^- by coal was calculated according to Equations (1) and (2), and the removal rate of NO_3^- by coal was calculated according to Equation (3):

$$q_e = \frac{V(C_0 - C_e)}{m} \tag{1}$$

$$q_t = \frac{V(C_0 - C_t)}{m} \tag{2}$$

$$RE = \frac{C_0 - C_e}{C_0} \times 100\% \tag{3}$$

where q_e is the amount of NO_3^- adsorbed by coal when the adsorption of NO_3^- reaches equilibrium, mg/g; q_t is the adsorption amount of NO_3^- adsorbed by coal at time t, mg/g; C_0 is the initial mass concentration of NO_3^-, mg/L; C_e is the mass concentration of N NO_3^- at adsorption equilibrium, mg/L; V is the volume of mine water, L; m is the mass of pulverized coal, g; RE is the removal rate of NO_3^-, %.

The pseudo-first-order kinetics [12], pseudo-second-order kinetics [13], and intra-particle diffusion models [14] were used to explore the steps of controlling the adsorption rate during the adsorption process, and the calculation formulas are described in Equations (4)–(6):

$$\lg(q_e - q_t) = \lg q_e - \frac{k_1 t}{2.303} \tag{4}$$

$$\frac{t}{q_t} = \frac{1}{k_2 q_e^2} + \frac{1}{q_e} \tag{5}$$

$$q_t = k_3 t^{1/2} + C \tag{6}$$

where k_1 is the pseudo-first-order adsorption rate constant, g/(mg·min); k_2 is the pseudo-second-order adsorption rate constant, g/(mg·min); k_3 is the rate constant of the internal diffusion model, g/(mg·min$^{-1/2}$); C is the boundary layer thickness, mg/g.

The Langmuir and Freundlich isothermal adsorption models were used to represent the solid–liquid equilibrium adsorption state, and the calculation formulas are described in Equations (7) and (8):

$$q_e = \frac{K_L q_m C_e}{1 + K_L C_e} \tag{7}$$

$$q_e = K_F C_e^{1/n} \tag{8}$$

where q_m is the monolayer saturated adsorption capacity of coal adsorbent, mg/g; K_L is the Langmuir adsorption equilibrium constant, L/mg; K_F is the Freundlich adsorption equilibrium constant, L/mg; n is the Freundlich constant.

2.4. Methods to Character the Mine Water

The TOC concentration in the water during the experiment was determined using a Shimadzu TOC–L CPH CN200 total organic carbon analyzer, and UV$_{254}$ was detected using a UV–visible spectrophotometer.

The concentration of the fluorescent components of DOM in mine water was determined using a dual-FL fluorescence spectrometer [15]. Millipore® pure water was used as a blank for fluorescence spectroscopy. The light source was a 150 W ozone-free xenon arc lamp. The excitation wavelength (Ex) and emission wavelength (EM) were within the range of 200–400 nm and 250–600 nm, respectively. The step size was increased by 5 nm. The scanning signal integration time was 3 seconds, and the system automatically corrected Rayleigh and Raman scattering.

The concentration of NO_3^- in the mine water was determined via ultraviolet spectrophotometry. Subsequently, the absorbance of NO_3^- solutions with concentrations of 5, 10, 15, 20, 25, 30, and 40 mg/L was measured using an ultraviolet spectrophotometer. The standard curve was drawn relative to the concentration of NO_3^-, and abscissa and absorbance were used as the ordinate, as shown in Figure 2.
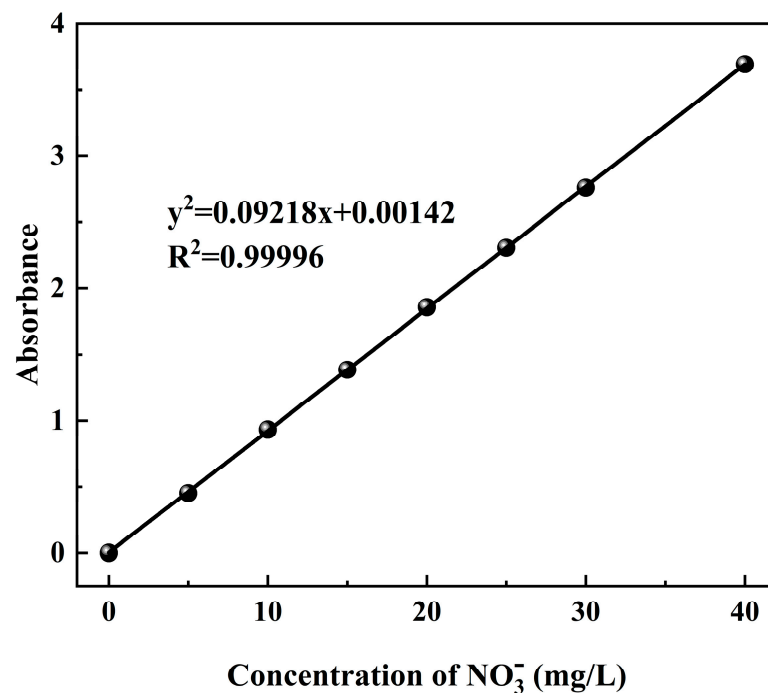
Figure 2. The NO_3^- measurement standard curve.

3. Results

3.1. Adsorption of NO_3^- in Mine Water by Residual Coal

Coal mine underground reservoir technology can effectively reduce the concentration of anions and cations in mine water. However, if the purified mine water still exceeds the emission standard for anions and cations, it may pose a potential environmental pollution risk. Apparently, NO_3^- stands out as a prominent pollutant within the water body. In case of its discharge into natural environments, there is a likelihood of elevated NO_3^- levels, leading to eutrophication phenomena in aquatic ecosystems. The ingestion of NO_3^-, whether directly or indirectly, poses a significant threat to human health. Therefore, monitoring the concentration of NO_3^- in the water body can provide valuable insights into its variation patterns and contribute to the analysis of factors influencing its concentration changes in mine water. In the dynamic simulation experiment of water–coal interactions, the initial concentration of NO_3^- was recorded as 124 mg/L. Over time, there was an initial decrease followed by a gradual increase in NO_3^- concentrations, ultimately reaching a final concentration of 92 mg/L and showing a downward trend, as shown in Figure 3.

Previous studies have demonstrated that coal, as a biological organic rock, contains kaolinite, calcite, and other minerals in addition to organic matter. These constituents are capable of reducing the levels of anions, cations, and heavy metal ions in water [16,17]. It is hypothesized that the substantial decrease in NO_3^- concentrations during the early stages of water–coal interactions can be attributed to the rapid adsorption of coal. Therefore, an adsorption experiment was conducted to investigate the effect of various factors (additional amount of residual coal, adsorption time, and initial concentration of NO_3^-) on the adsorptive capacity of residual coal towards NO_3^-. The results of NO_3^- adsorption in residual coal under different conditions are shown in Figure 4.
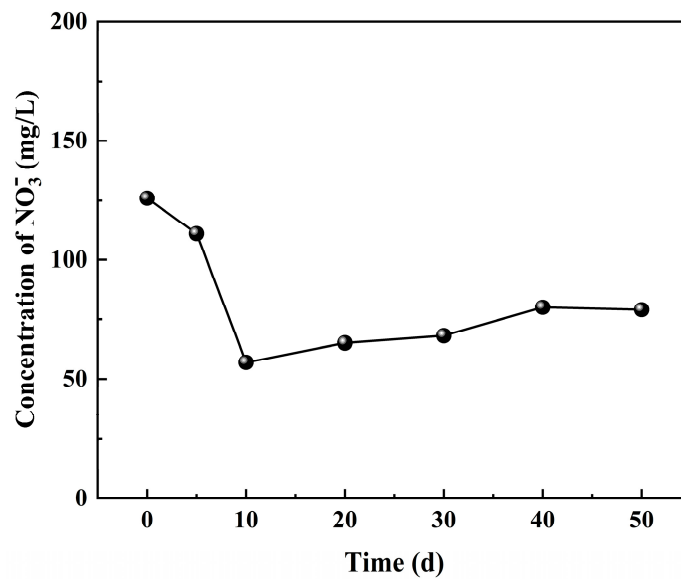
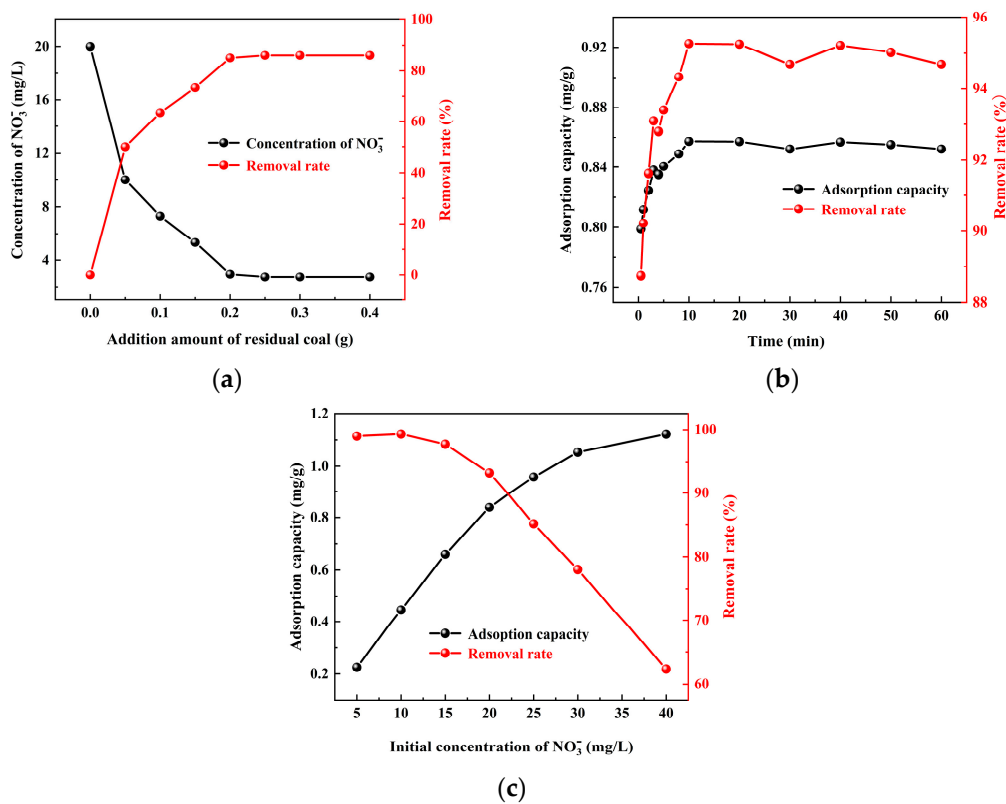**Figure 3.** The variation in NO_3^- concentrations with time during the water–coal interaction process.

Figure 4. The adsorption capacity and removal rate of NO_3^- on residual coal under different adsorption conditions: (**a**) additional amount of residual coal, (**b**) adsorption time, and (**c**) initial concentration of NO_3^-.

The effect of coal dosage on the adsorption and removal of NO_3^- in the mine water by coal is shown in Figure 4a. The concentration of NO_3^- in the mine water decreased with an increase in coal dosage, leading to an increase in the removal rate. When the dosage exceeded 0.2 g, the coal achieved an impressive removal rate of 85% with respect to NO_3^-. The relationship between the adsorption time and adsorption capacity, as well as the removal rate of NO_3^- in residual coal, is shown in Figure 4b. Within the time range of 0.5–10 min, a significant variation in the removal rate of NO_3^- by coal was observed, reach-

ing up to 95%, followed by a relatively stable trend. The effect of the initial concentration of the NO_3^- solution with respect to the adsorption and removal process by coal is shown in Figure 4c. The adsorption capacity of NO_3^- by coal increased with an increase in the initial concentration of NO_3^-. When the initial concentration ranges from 5 to 15 mg/L, the removal rate of NO_3^- by coal can reach high levels of 97.7–99.3%. However, as the initial concentration of the NO_3^- solution further increased, the removal rate gradually decreased. These findings indicate that the coal dosage, constant temperature oscillation time, and initial concentration of the NO_3^- solution all significantly influence the adsorption of NO_3^- by coal. Moreover, during the course of the adsorption reaction, there was a gradual increase in the amount of NO_3^- adsorbed by coal until it reached dynamic equilibrium. The observed variations in NO_3^- concentrations under different adsorption conditions aligned with the conclusions of previous researchers.

Based on the above, it can be inferred that the primary factors influencing the adsorption of NO_3^- by coal under varying conditions are primarily attributed to the total specific surface area and adsorption sites present on the surface of pulverized coal. The augmentation in coal dosage leads to an increase in both the total specific surface area and adsorption sites of coal particles, thereby resulting in an elevated removal rate of NO_3^- by coal. With the extension of oscillation times, a majority of vacant adsorption sites on the surface of coal particles become occupied by NO_3^-, consequently causing no alteration in both the adsorption rate and removal rate of NO_3^- by residual coal. Furthermore, elevating the initial concentration of NO_3^- within mine water effectively enhances effective collisions with the blank surfaces of coal, facilitating a complete reaction between NO_3^- within mine water and coal surfaces while augmenting the adsorption capacity for NO_3^- by coal.

3.2. Adsorption Mechanism of Residual Coal on NO_3^- in Mine Water

To further investigate the adsorption mechanism of coal on NO_3^-, adsorption kinetics was studied based on the experimental data. Adsorption kinetics plays a crucial role in understanding the rate-controlling steps involved in the adsorption process and is of significant importance for studying this phenomenon. The construction of an adsorption kinetics model can provide detailed insights into the dynamic behavior of static adsorption and facilitate a comprehensive analysis of the entire adsorption process.

The adsorbate–adsorbent interaction during the adsorption process can be divided into three processes [18]:

(a) Membrane diffusion refers to the process of adsorbate molecules diffusing through a thin liquid layer on the surface of an adsorbent.
(b) Intraparticle diffusion refers to the diffusion of adsorbate molecules in the solution of fine pores (i.e., fine pore diffusion), followed by further diffusion at the solid–liquid interface of the inner surface (known as inner surface diffusion).
(c) Adhesion refers to the process in which the adsorbate migrates towards the inner surface and forms a bond with specific adsorption sites on the solid surface under the action of attractive force.

The kinetic equation of NO_3^- adsorptions in the coal mine water was simulated using pseudo-first-order kinetics, pseudo-second-order kinetics, and intraparticle diffusion models. The kinetic model's fitting curves are shown in Figure 5, and kinetic-related parameters are shown in Table 1.

The results presented in Table 1 demonstrate that the correlation coefficient (0.2824) for the pseudo-first-order kinetics model was comparatively lower than the correlation coefficient (0.9999) obtained for the pseudo-second-order kinetics model, indicating that the adsorption process of NO_3^- by coal in the mine water adheres to the pseudo-second-order kinetics model and suggesting a chemical adsorption mechanism [19]. The calculated value q_e (calc) in the pseudo-second-order kinetics model closely aligned with the experimental value q_e (meas), providing further evidence that the adsorption process of NO_3^- by coal adhered to the pseudo-second-order kinetics model. This finding also confirmed that the adsorption site on the coal surface significantly influenced the adsorption of NO_3^- by

coal, thereby validating the correctness of the inference. The correlation coefficient of the intraparticle diffusion model can be utilized to assess the impact of liquid film diffusion and particle internal diffusion on the adsorption rate [20]. Within the framework of the intraparticle diffusion model, the adsorption process of NO_3^- by coal in the mine water can be divided into three distinct stages. The initial stage is associated with membrane diffusion, followed by an intraparticle diffusion stage, and ultimately culminating in an equilibrium dynamic stage encompassing both adsorption and desorption processes. The correlation coefficients for the three stages were 0.9739, 0.9137, and 0.2446. The higher correlation coefficients observed in the first two stages suggested that intraparticle diffusion also played a role in the adsorption process of coal to NO_3^-. Furthermore, the nonzero intercepts indicated that the fitted curves do not intersect with the origin. It can be observed that the reaction rate was controlled by both membrane diffusion and intraparticle diffusion [21,22]. The slopes of the first and second stages of the straight line in Figure 5c indicated rapid membrane diffusion and internal diffusion during the initial adsorption process. At the same time, it is also consistent with the change in the NO_3^- adsorption rate of coal in Figure 4c. However, according to Table 1, the correlation coefficient for the first stage was higher than that for the second stage, indicating that membrane diffusion plays a dominant role in controlling the adsorption rate.
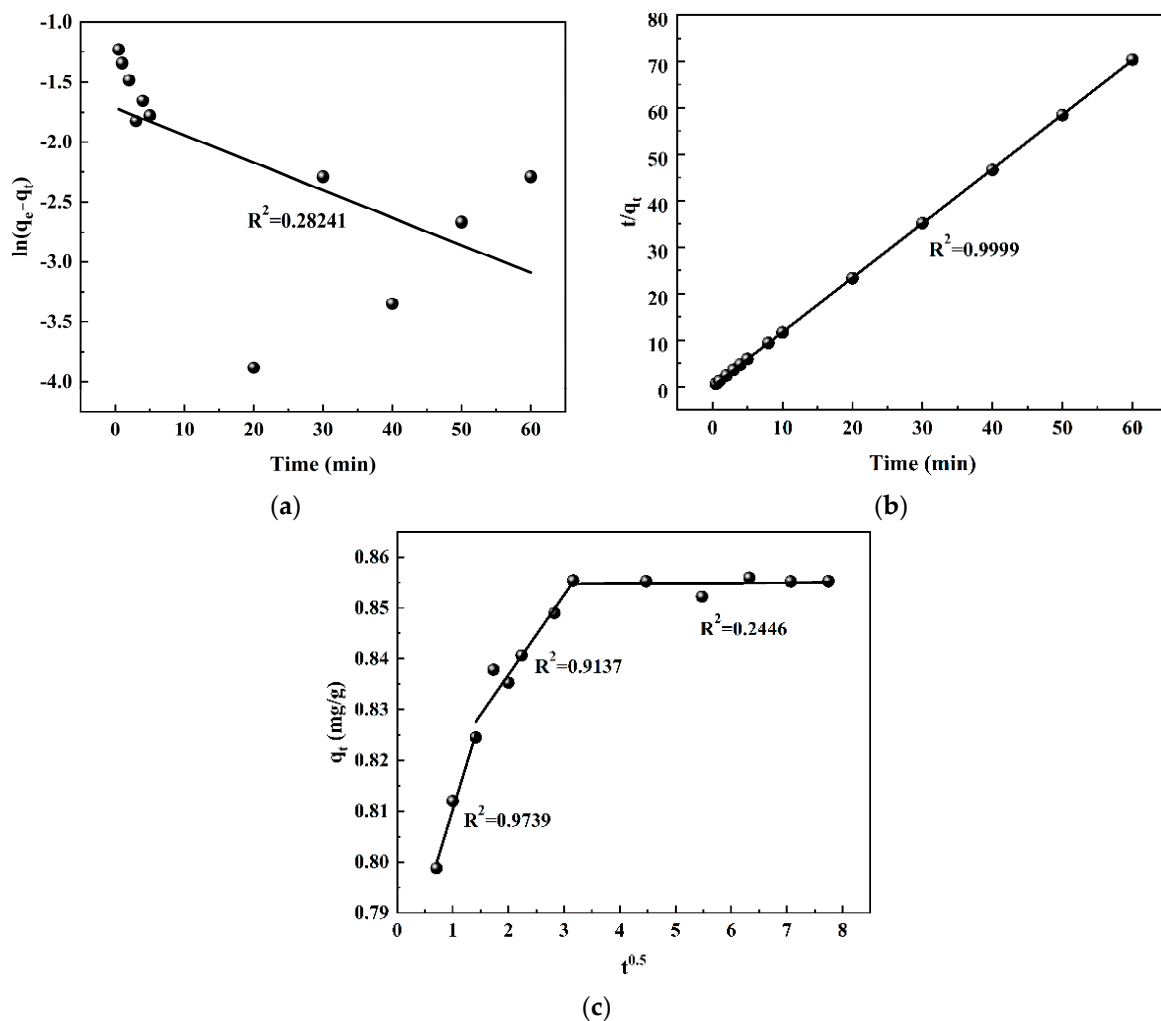
Figure 5. The fitting results of NO_3^- adsorption kinetics on residual coal under different kinetic models: (**a**) pseudo-first-order kinetics, (**b**) pseudo-second-order kinetics, and (**c**) intraparticle diffusion model.
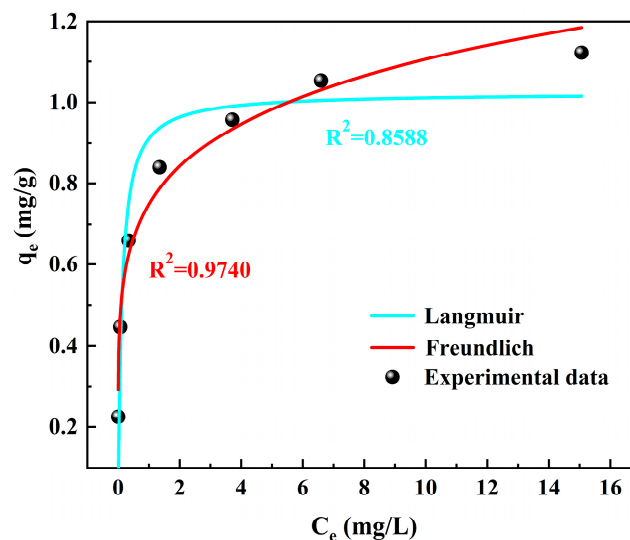
Table 1. Parameters of NO_3^- adsorption kinetics on residual coal under pseudo-first-order kinetics, pseudo-second-order kinetics, and intraparticle diffusion models.

Pseudo-First-Order				Pseudo-Second-Order			Intraparticle Diffusion Model								
q_e (Meas *) (mg/g)	q_e (Calc #) (mg/g)	k_1	R^2	q_e (Calc) (mg/g)	k_2	R^2	k_{31}	Intercept	R^{12}	k_{32}	Intercept	R^{22}	k_{33}	Intercept	R^{32}
0.8574	0.01933	0.05276	0.2824	0.8549	27.8212	0.9999	0.03601	0.7743	0.9739	0.03450	0.8054	0.9137	0.01572	0.8546	0.2446

* means value by experiment; # calc means value by calculation.

To gain a deeper understanding of the interaction between residual coal and NO_3^-, as well as to clarify the adsorption mechanism of residual coal towards NO_3^-, an adsorption isotherm simulation study was carried out. The isothermal adsorption process was fitted using Langmuir and Freundlich isotherms based on the adsorption data of NO_3^- on coal [23], as shown in Figure 6. The saturated adsorption capacity and adsorption constant of NO_3^- on coal were calculated using linear regression analysis, as shown in Table 2.

Figure 6. The fitting results of NO_3^- adsorption isotherms on residual coal under Langmuir and Freundlich models.

Table 2. Parameters of NO_3^- adsorption isotherms on residual coal using Langmuir and Freundlich models.

Langmuir			Freundlich		
K_L (L/mg)	q_m (mg/g)	R_2	K_F (L/mg)	$1/n$	R^2
8.0648	1.0239	0.8588	0.7487	0.1695	0.9740

By comparing the correlation coefficient, it can be observed that the adsorption of NO_3^- in the mine water by coal conforms more closely to the Freundlich isotherm model, indicating a heterogeneous layer adsorption process for NO_3^- in the mine water by coal [24]. Furthermore, the value of $1/n$ in the fitting equation (0.1695) was less than 1 and suggested a strong interaction between coal and NO_3^-, facilitating the adsorption process.

3.3. Variation Law of Dissolved Organic Matter in Mine Water

The concentration of NO_3^- in mine water decreased during the initial 0–10 days of water–coal interactions due to the adsorption of NO_3^- by residual coal. However, after 10 days, the concentration of NO_3^- began to increase slightly, as shown in Figure 3. Dissolved organic matter contains macromolecular organic nitrogen, which can be converted

into inorganic nitrogen under the action of microorganisms (that is, the mineralization of organic nitrogen), thereby influencing the distribution and content of nitrogen. Tang et al. [25] investigated the transformation of DOM and nitrogen during an anaerobic/anoxic/oxic process carried out using fluorescence spectroscopy, revealing that the mineralization of DOM occurred during the oxidation process and further leading to its conversion into ammonia nitrogen.

The content of TOC and the value of UV_{254} in mine water were measured on the 0th, 10th, 20th, and 50th day of the dynamic simulation experiment, as shown in Table 3. On the 0th day of the simulation experiment, the TOC content in the mine water at the inlet of the coal mine underground reservoir was determined to be 15.33 mg/L. Following the reaction, a decrease in TOC content to 8.31 mg/L was observed with a removal rate reaching 45.79%. The value of UV_{254} in the water was measured at 0.17 cm^{-1}, while it decreased to 0.02 cm^{-1} after the reaction, indicating an 88.24% reduction. This suggested that the water–coal interaction could effectively remove humic macromolecular organic matter from the water, aligning with observed changes in the underground reservoir of the Daliuta Coal Mine. The values of TOC and UV_{254} used to characterize DOM at the outlet of the underground reservoir in the Daliuta coal mine were lower than those in the inlet, indicating a downward trend in DOM concentrations within the water body. It is hypothesized that the macromolecular organic nitrogen contained in the mine water can be transformed into NO_2^- under the action of microorganisms, which subsequently oxidized to NO_3^-, thereby increasing the concentration of NO_3^- in the water body.

Table 3. Chemical characteristics of mine water at different times during the water–coal interaction process.

Time	TOC (mg/L)	UV_{254} (cm^{-1})
0th day	15.33	0.17
10th day	12.16	0.14
20th day	9.07	0.09
50th day	8.31	0.02

The decrease in TOC and UV_{254} values in the mine water indicated a declining trend of DOM under the action of water–coal interactions. However, it failed to analyze the variation in each component of DOM with time. Therefore, the three-dimensional fluorescence spectrum was used to distinguish the components of DOM in mine water at different time points, which can clarify the variation in individual components of DOM that are influenced by water–coal interactions [26,27].

The three-dimensional fluorescence spectra of mine water samples at different times during the dynamic simulation experiment are shown in Figure 7, while the positions and intensities of the fluorescence peaks in these spectra are shown in Table 4. To better understand the fluorescence characteristics of mine water during the experiment, the entire spectral range was divided into five distinct regions [28,29]: tyrosine region I (EX 200–250/EM 240–330), tryptophan region II (EX 200–250/EM 330–380), fulvic acid region III (EX 200–250/EM 380–600), soluble microbial product region IV (EX 250–400/EM 240–380), and humic acid region V (EX 250–400/EM 380–600).

The tryptophan zone II in mine water was attributed to a protein-like substance, and its fluorescence intensity exhibited significance during the early stage of the reaction. Tryptophan primarily originates from the decomposition of residues, such as microorganisms and phytoplankton, in water, along with extracellular enzymes secreted by microorganisms [30], indicating that mine water is influenced by human activities or microorganisms. From Table 4, it can be observed that the fluorescence intensity of tryptophan in mine water before the reaction was 425.1, while it reduced to 195.1 after undergoing the dynamic simulation testing, indicating that the water–coal interaction had an excellent removal effect on tryptophan in mine water, which aligned with the results of TOC and UV_{254} analysis. During the experiment, the fluorescence intensity of region I and region II decreased, while

the fluorescence intensity of region III in mine water increased slightly after 30 days of reaction, which exhibited a reduction in protein substances and an elevation in fulvic acid substances within the mine water. Furthermore, it indicated that the DOM in mine water was influenced by microorganisms, leading to the production of small amounts of humus substances during protein degradation. Consequently, the increase in NO_3^- concentrations in the process of the water–coal interaction experiment came from the mineralization of nitrogen-containing macromolecular organic matter, such as tryptophan, in water. Under the action of microorganisms in water, tryptophan and other protein substances were hydrolyzed into NO_3^-, thereby increasing their concentrations in mine water.
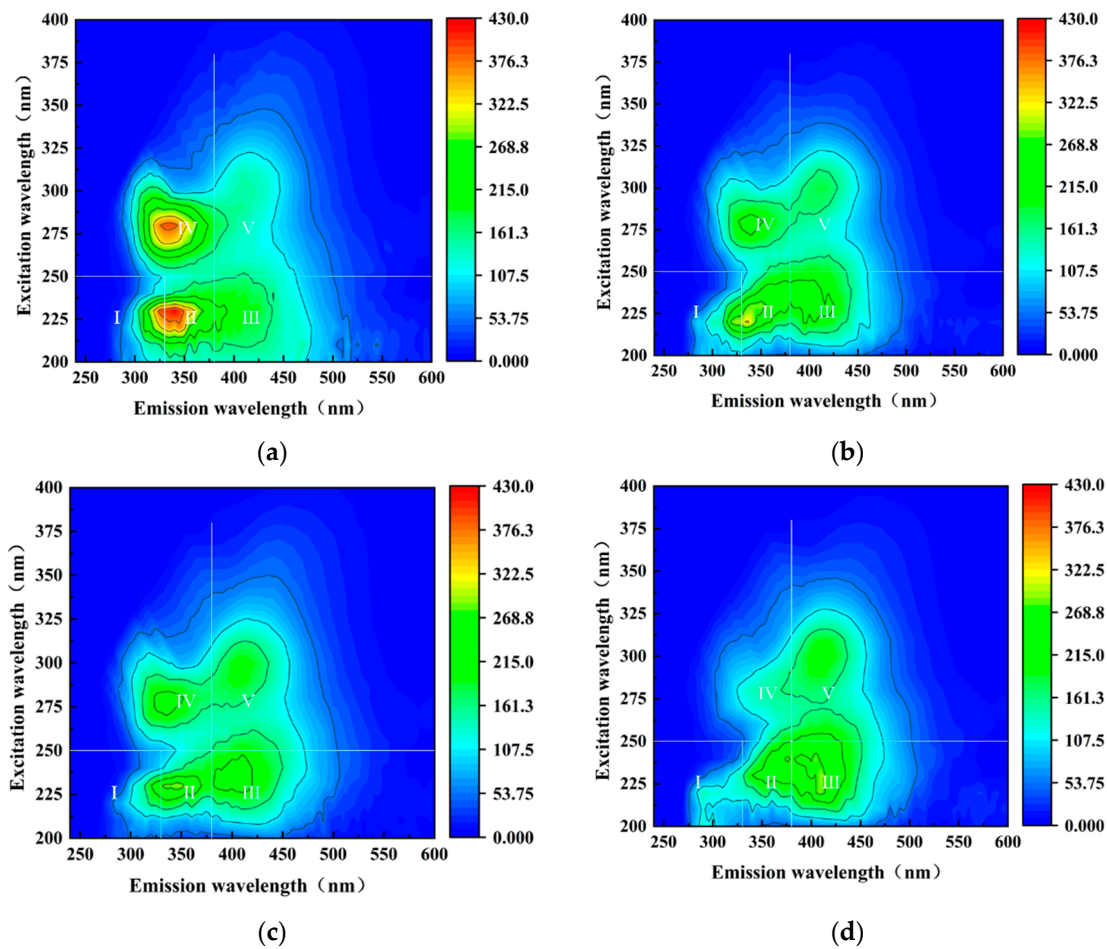
Figure 7. DOM fluorescence spectra of mine water at different times during the water–coal interaction process: (**a**) 0th, (**b**) 10th, (**c**) 20th, and (**d**) 50th day.

Table 4. Location and intensity of DOM fluorescence peaks in mine water at different times.

Time	λ EX/EM (nm)	Fmax
0th day	230/335 280/335	425.1 393.2
10th day	220/335 280/340	331.2 241.7
20th day	230/345 280/335 230/405	293.5 246.6 240.7
50th day	230/340	195.1

4. Discussion

The decomposition and transformation process of organic nitrogen can be divided into two stages. Firstly, under the influence of microbial enzymes, nitrogen-containing compounds, such as various complex proteins and amino acids, rich in water are gradually hydrolyzed to generate simpler amino compounds. Secondly, with the further participation of microorganisms, nitrogen-containing compounds are transformed to release ammonia. Under anoxic conditions, microorganisms ceased to decompose and convert ammonia. Ammonia is the final degradation product of organic nitrogen under anoxic conditions. However, when there is a certain amount of oxygen in the water, ammonia can be further oxidized into nitrite due to nitrifying bacteria, and it is ultimately converted into nitrate.

The concentration of NO_3^- in mine water decreased significantly within the first 0–10 days under the influence of water–coal interactions, which were caused by the adsorption of the coal pillar dam and residual coal in goaf. Subsequently, the concentration of NO_3^- gradually increased. The increase in NO_3^- concentrations in mine water can be attributed to the presence of organic pollutants originating from coal mine underground reservoirs, including emulsion, organic animals and plants, and oil pollution. These organic pollutants all contained macromolecular organic nitrogen that can undergo microbial-mediated conversion into ammonia. In the presence of oxygen, ammonia was oxidized to NO_2^- by nitrite bacteria. Subsequently, NO_2^- was converted into NO_3^- eventually, leading to an increase in the concentration of NO_3^- in mine water, as shown in Figure 8. Although the dynamic simulation experimental device of the water–coal interaction accurately simulates the flow conditions of mine water in coal mine underground reservoirs, the actual operation of the underground reservoir of the coal mine was carried out under aerobic conditions without controlling oxygen contents. Consequently, during the actual operation of underground coal mine reservoirs in anoxic states, a greater proportion of N in the mine water was converted into NH_4^+.
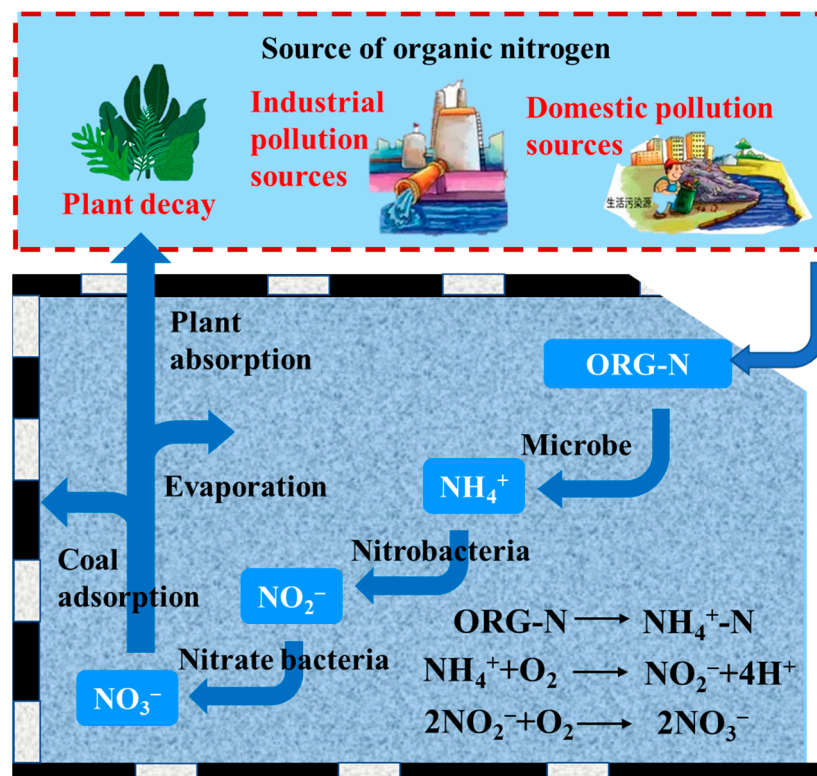

Figure 8. Schematic diagram of the nitrogen cycle in mine water under the action of water coal.

5. Conclusions

The initial decrease in NO_3^- concentrations during the water–coal interaction was attributed to coal adsorption. According to the adsorption data of NO_3^- with respect to coal, the adsorption kinetics and isothermal adsorption model's calculations were carried out. The R^2 of the pseudo-second-order kinetic model in the adsorption kinetics was higher than that of the pseudo-first-order kinetic model, indicating that the adsorption process of NO_3^- on coal was chemical adsorption. The intraparticle diffusion model was divided into three stages for fitting, and the intercepts in the three stages were not 0, indicating that both the membrane diffusion process and the intraparticle diffusion jointly control the reaction rate. The R^2 of the Freundlich isotherm adsorption model was higher than that of the Langmuir model, indicating that the adsorption process of coal on NO_3^- in mine water comprises heterogeneous layer adsorption. Moreover, the value of $1/n$ in the Freundlich isotherm adsorption equation was less than 1, further supporting an easy occurrence of NO_3^- adsorptions in coal.

The increase in NO_3^- concentration after 10 days of water–coal interactions was attributed to the hydrolysis of organic nitrogen, leading to the conversion of nitrogen-containing organic matter into NO_3^- and subsequently elevating its content in water. The composition and fluorescence peak intensity of DOM in mine water samples at different times were observed using three-dimensional fluorescence spectroscopy. Remarkable changes were observed in the fluorescence intensity of tryptophan region II in DOM, decreasing from 425.1 before the reaction to 195.1. Tryptophan, as a protein-like substance rich in nitrogen, can be mineralized by microorganisms into inorganic nitrogen compounds. Therefore, it can be inferred that the involvement of microorganisms facilitated the hydrolysis of proteins such as tryptophan in mine water, resulting in an increase in NO_3^- concentrations.

Author Contributions: Conceptualization, B.J. and D.L. (Dingcheng Liang); methodology, Z.Z. and D.L. (Dingcheng Liang); validation, Z.C., J.T., H.Z. and Y.L.; formal analysis, Z.Z. and D.L. (Dingcheng Liang); investigation, B.J. and Z.Z.; resources, B.J.; data curation, D.L. (Dingcheng Liang); writing—original draft preparation, Z.Z. and D.L. (Deqian Liu); writing—review and editing, D.L. (Dingcheng Liang) and Y.L.; supervision, D.L. (Dingcheng Liang) and Y.L.; project administration, D.L. (Dingcheng Liang). All authors have read and agreed to the published version of the manuscript.

Data Availability Statement: All data generated or analyzed during this study are included in this published article.

Conflicts of Interest: The authors declare no conflict of interest.

References

1. Zhang, C.; Wang, F.T.; Bai, Q.S. Underground space utilization of coalmines in China; a review of underground water reservoir construction. *Tunn. Undergr. Space Technol.* **2021**, *107*, 103657. [CrossRef]
2. Chen, Z.; Zhao, X.; Han, Z.; Ji, Y.; Qiao, Z. Reasonable size design and influencing factors analysis of the coal pillar dam of an underground reservoir in Daliuta mine. *Processes* **2023**, *11*, 2006. [CrossRef]
3. Cameira, M.R.; Rolim, J.; Valente, F.; Mesquita, M.; Dragosits, U.; Cordovil, C.M.d.S. Translating the agricultural N surplus hazard into ground-water pollution risk: Implications for effectiveness of mitigation measures in nitrate vulnerable zones. *Agr. Ecosyst. Environ.* **2021**, *306*, 107204. [CrossRef]
4. Fetisov, V.; Gonopolsky, A.M.; Davardoost, H.; Ghanbari, A.R.; Mohammadi, A.H. Regulation and impact of VOC and CO_2 emissions on low-carbon energy systems resilient to climate change: A case study on an environmental issue in the oil and gas industry. *Energy Sci. Eng.* **2023**, *11*, 1516–1535. [CrossRef]
5. Wang, S.; Chen, J.; Zhang, S.X.; Zhang, X.Y.; Chen, D.; Zhou, J. Hydrochemical evolution characteristics, controlling factors, and high nitrate hazards of shallow groundwater in a typical agricultural area of Nansi Lake Basin, North China. *Environ. Res.* **2023**, *223*, 115430. [CrossRef] [PubMed]
6. Zhao, L.; Sun, Y.F.; Yang, Z.B.; Wang, S.D.; Yang, J.; Sun, C.; Tian, Y.F. Removal efficiencies of dissolved organic matter and ammonium in coal mine water by coal gangue through column experiments. *J. China Coal Soc.* **2018**, *43*, 236–241. (In Chinese)

7. Zhang, Q.; Luo, S.H.; Zhao, L.; Wang, S.D.; Tian, Y.F.; Zhang, L.; Meng, J.; Zhang, Z.J. Migration and transformation regulation of organic and inorganic nitrogen in a western coal mine groundwater reservoir. *J. China Coal Society* **2019**, *44*, 899–905. (In Chinese)

8. Xiong, Y.J.; Du, Y.; Deng, Y.M.; Ma, T.; Li, D.; Sun, X.L.; Liu, G.N.; Wang, Y.X. Contrasting sources and fate of nitrogen compounds in different groundwater systems in the Central Yangtze River Basin. *Environ. Pollut.* **2021**, *290*, 118119. [CrossRef]

9. Mladenov, N.; Parsons, D.; Kinoshita, A.M.; Pinongcos, F.; Mueller, M.; Garcia, D.; Lipson, D.A.; Grijalva, L.M.; Zink, T.A. Groundwater-surface water interactions and flux of organic matter and nutrients in an urban, Mediterranean stream. *Sci. Total Environ.* **2022**, *811*, 152379. [CrossRef]

10. *HJ494–2009*; Water Quality—Guidance on Sampling Techniques. National Environmental Protection Standards of the People's Republic of China. Ministry of Ecology and Environment of the People's Republic of China: Beijing, China, 2009. (In Chinese)

11. *HJ495–2009*; Water Quality—Technical Regulation on the Design of Sampling Programmes. National Environmental Protection Standards of the People's Republic of China. Ministry of Ecology and Environment of the People's Republic of China: Beijing, China, 2009. (In Chinese)

12. Kim, Y.S.; Kim, J.H. Isotherm, kinetic and thermodynamic studies on the adsorption of paclitaxel onto Sylopute. *J. Chen. Thermodyn.* **2019**, *130*, 104–113. [CrossRef]

13. Hallajiqomi, M.; Eisazadeh, H. Adsorption of manganese ion using polyaniline and it's nanocomposite: Kinetics and isotherm studies. *J. Ind. Eng. Chem.* **2017**, *55*, 191–197. [CrossRef]

14. Selim, A.Q.; Mohamed, E.A.; Mobarak, M.; Zayed, A.M.; Seliem, M.K.; Sridhar Komarneni, S. Cr(VI) uptake by a composite of processed diatomite with MCM-41: Isotherm, kinetic and thermodynamic studies. *Micropor. Mesopor. Mat.* **2018**, *260*, 84–92. [CrossRef]

15. Yuan, D.H.; Guo, X.J.; Wen, L.; He, L.S.; Wang, J.G.; Li, J.Q. Detection of Copper (II) and Cadmium (II) binding to dissolved organic matter from macrophyte decomposition by fluorescence excitation-emission matrix spectra combined with parallel factor analysis. *Environ. Pollut.* **2015**, *204*, 152–160. [CrossRef]

16. Wang, Y.H.; Yang, W.; Lin, B.Q.; Yan, F.Z. Effects of different conductive ions on pore-structure evolution of medium and high-rank coal bodies induced by electric pulses. *Fuel* **2021**, *293*, 1–9. [CrossRef]

17. Braik, S.; Amor, T.B.; Michelin, L.; Rigolet, S.; Bonne, M.; Lebeau, B.; Hafiane, A. Natural water defluoridation by adsorption on Laponite clay. *Water Sci. Technol.* **2022**, *85*, 1701–1719. [CrossRef] [PubMed]

18. Pan, W.L.; Xie, H.M.; Zhou, Y.; Wu, Q.Y.; Zhou, J.Q.; Guo, X. Simultaneous adsorption removal of organic and inorganic phosphorus from discharged circulating cooling water on biochar derived from agricultural waste. *J. Clean. Prod.* **2023**, *383*, 135496. [CrossRef]

19. Dim, P.E.; Mustapha, L.S.; Termtanun, M.; Okafor, J.O. Adsorption of chromium (VI) and iron (III) ions onto acid-modified kaolinite: Isotherm, kinetics and thermodynamics studies. *Arab. J. Chem.* **2021**, *14*, 103064. [CrossRef]

20. Wang, J.L.; Guo, X. Rethinking of the intraparticle diffusion adsorption kinetics model: Interpretation, solving methods and applications. *Chemosphere* **2022**, *309*, 136732. [CrossRef]

21. Inglezakis, V.J.; Fyrillas, M.M.; Park, J. Variable diffusivity homogeneous surface diffusion model and analysis of merits and fallacies of simplified adsorption kinetics equations. *J. Hazard. Mater.* **2019**, *367*, 224–245. [CrossRef] [PubMed]

22. Danish, M.; Ansari, K.B.; Danish, M.; Khatoon, A.; Rao, R.A.K.; Zaidi, A.; Aftab, R.A. A comprehensive investigation of external mass transfer and intraparticle diffusion for batch and continuous adsorption of heavy metals using pore volume and surface diffusion model. *Sep. Purif. Technol.* **2022**, *292*, 120996. [CrossRef]

23. Baseri, H.; Tizro, S. Treatment of nickel ions from contaminated water by magnetite based nanocomposite adsorbents: Effects of thermodynamic and kinetic parameters and modeling with Langmuir and Freundlich isotherms. *Process Saf. Environ. Prot.* **2017**, *109*, 465–477. [CrossRef]

24. Iwuozor, K.O.; Oyekunle, I.P.; Emenike, E.C.; Okoye-Anigbogu, S.M.; Ibitogbe, E.M.; Elemile, O.; Ighalo, J.O.; Adeniyi, A.G. An overview of equilibrium, kinetic and thermodynamic studies for the sequestration of Maxilon dyes. *Clean. Mat.* **2022**, *6*, 100148. [CrossRef]

25. Tang, G.; Li, B.R.; Zhang, B.W.; Wang, C.; Zeng, G.C.; Zheng, X.; Liu, C.X. Dynamics of dissolved organic matter and dissolved organic nitrogen during anaerobic/anoxic/oxic treatment processes. *Bioresour. Technol.* **2021**, *331*, 125026. [CrossRef] [PubMed]

26. Lu, K.T.; Gao, H.J.; Yu, H.B.; Liu, D.P.; Zhu, N.M.; Wan, K.L. Insight into variations of DOM fractions in different latitudinal rural black-odor waterbodies of eastern China using fluorescence spectroscopy coupled with structure equation model. *Sci. Total Environ.* **2022**, *816*, 151531. [CrossRef] [PubMed]

27. Ma, L.X.; Li, B.; Yabo, S.D.; Li, Z.; Qi, H. Fluorescence fingerprinting characteristics of water-soluble organic car-bon from size-resolved particles during pollution event. *Chemosphere* **2022**, *307*, 135748. [CrossRef]

28. Liu, F.; Zhao, Q.L.; Ding, J.; Li, L.L.; Wang, K.; Zhou, H.M.; Jiang, M.; Wei, J. Sources, characteristics, and in situ degradation of dissolved organic matters: A case study of a drinking water reservoir located in a cold-temperate forest. *Environ. Res.* **2023**, *217*, 114857. [CrossRef] [PubMed]

29. Zhang, L.; Sun, Q.X.; Dou, Q.H.; Lan, S.; Peng, Y.Z.; Yang, J.C. The molecular characteristics of dissolved organic matter in urbanized river sediments and their environmental impact under the action of microorganisms. *Sci. Total Environ.* **2022**, *827*, 154289. [CrossRef] [PubMed]

30. Malits, A.; Monforte, C.; Iachetti, C.; Gerea, M.; Latorre, M. Source characterization of dissolved organic matter in the eastern Beagle Channel from a spring situation. *J. Marine Syst.* **2023**, *240*, 103863. [CrossRef]